

PhysEmbedFormer: A Physics-Guided Interpretable Architecture for Medium-Term Forecasting of PV Power

Supplementary Material

Yue Yu¹, Pavel Loskot², Yu Gao³

¹ College of Information Science and Electronic Engineering, Zhejiang University, Hangzhou 310058, China

² Zhejiang University - University of Illinois Urbana-Champaign Institute, Zhejiang University, Haining 314400, China

³ AI Research Center, Midea Group, Shanghai 201103, China

List of supplementary figures

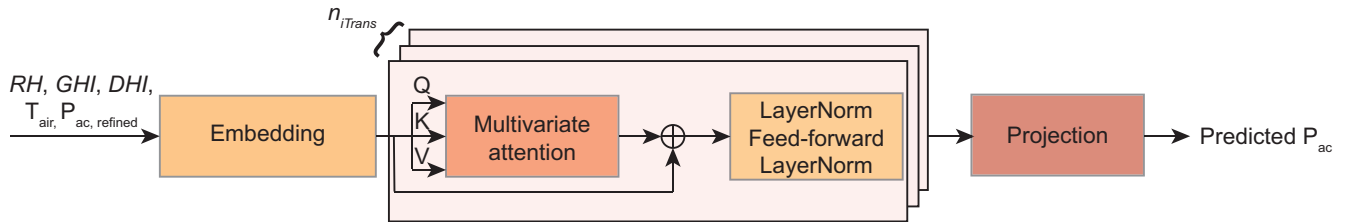
Figure S1. A block diagram of the iTransformer for forecasting time series.	2
Figure S2. The physics-guided decomposition of the PV power time series.	3
Figure S3. The learned values of α_{physics} and α_{residual} at different sites.	3
Figure S4. The L_1 and L_2 norms of the B-spline weights at the first KAN module.	4
Figure S5. The L_1 and L_2 norms of the B-spline weights at the second KAN module.	4

List of supplementary tables

Table S1. The key variables and parameters of PhysEmbedFormer	2
Table S2. Configuration of numerical experiments	2
Table S3. The ablation experiments for the dataset at site 10	5
Table S4. The ablation experiments for the dataset at site 11	5
Table S5. The ablation experiments for the dataset at site 17	6
Table S6. The ablation experiments for the dataset at site 19	6

Table S1. The key variables and parameters of PhysEmbedFormer

Symbol	Unit	Type	Description
P_{ac}	kW	objective variable	The actual electrical power generated by the PV array at each time step
T_{air}	$^{\circ}C$	auxiliary variable	The temperature of the PV array
RH	%	auxiliary variable	The percentage of the actual amount of water vapor in the air compared to the maximum amount the air can hold at that temperature
GHI	Wh/m^2	auxiliary variable	The total amount of solar radiation received by a horizontal surface
DHI	Wh/m^2	auxiliary variable	The component of solar radiation that reaches the Earth's surface after being scattered by the atmosphere
P_{rated}	kW	auxiliary constant	The total rated power output of the PV array under Standard Test Conditions (STC)
β	deg	auxiliary constant	The tilt of the PV array, positive if the array is in the Southern Hemisphere and tilts positively toward the geographic north
α	deg	auxiliary constant	The azimuth of the PV array, measured clockwise from the Solar North, with 0° being north, 90° east, 180° south, and 270° west
ρ_g	[-]	auxiliary constant	The fraction of incident solar radiation reflected by the Earth's surface
γ	$1/^{\circ}C$	auxiliary constant	Temperature coefficient that is generally negative, and quantifies the percentage decrease in output per $^{\circ}C$
η	[-]	auxiliary constant	The energy conversion efficiency of an inverter in the process of converting direct current (DC) to alternating current (AC)
P_{max}	kW	auxiliary constant	The maximum output AC power of the inverter

**Figure S1.** A block diagram of the iTransformer for forecasting time series.**Table S2.** Configuration of numerical experiments

Parameter	Value
GPU	NVIDIA GeForce RTX 4060
Batch size	128
# epochs	150
Initial learning rate	10^{-3}
Optimizer	Adam
window lengths (L_p, L_h)	(24,4), (48,12), (72,24), (96,48), (120,72)
training : validation : testing data split	8 : 1 : 1

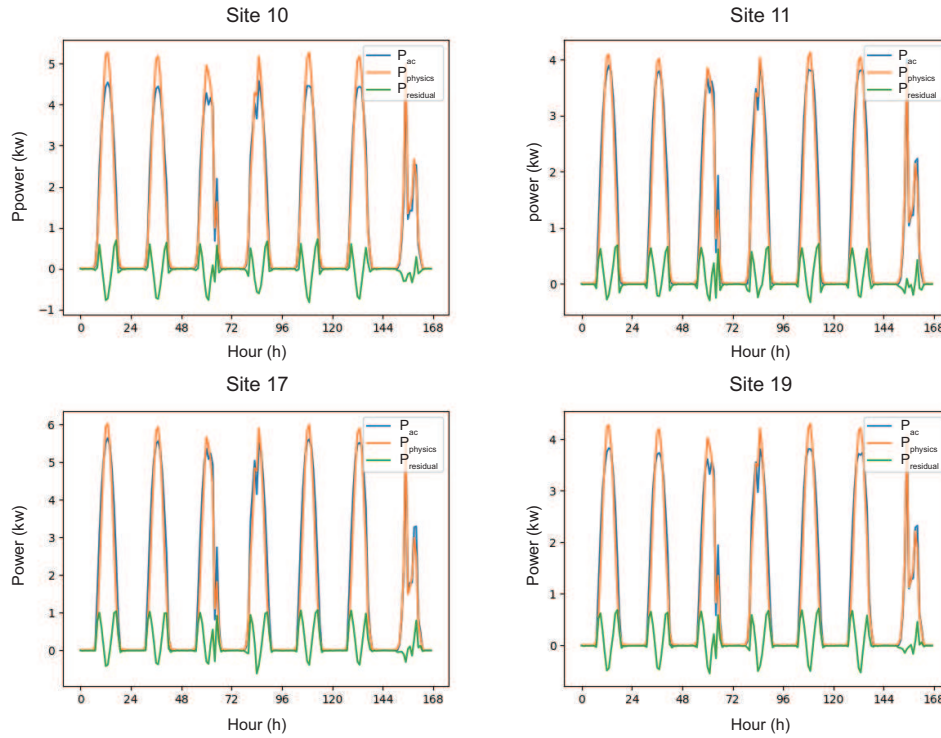


Figure S2. The physics-guided decomposition of the PV power time series into two components over 168 hours, for the four sites considered.

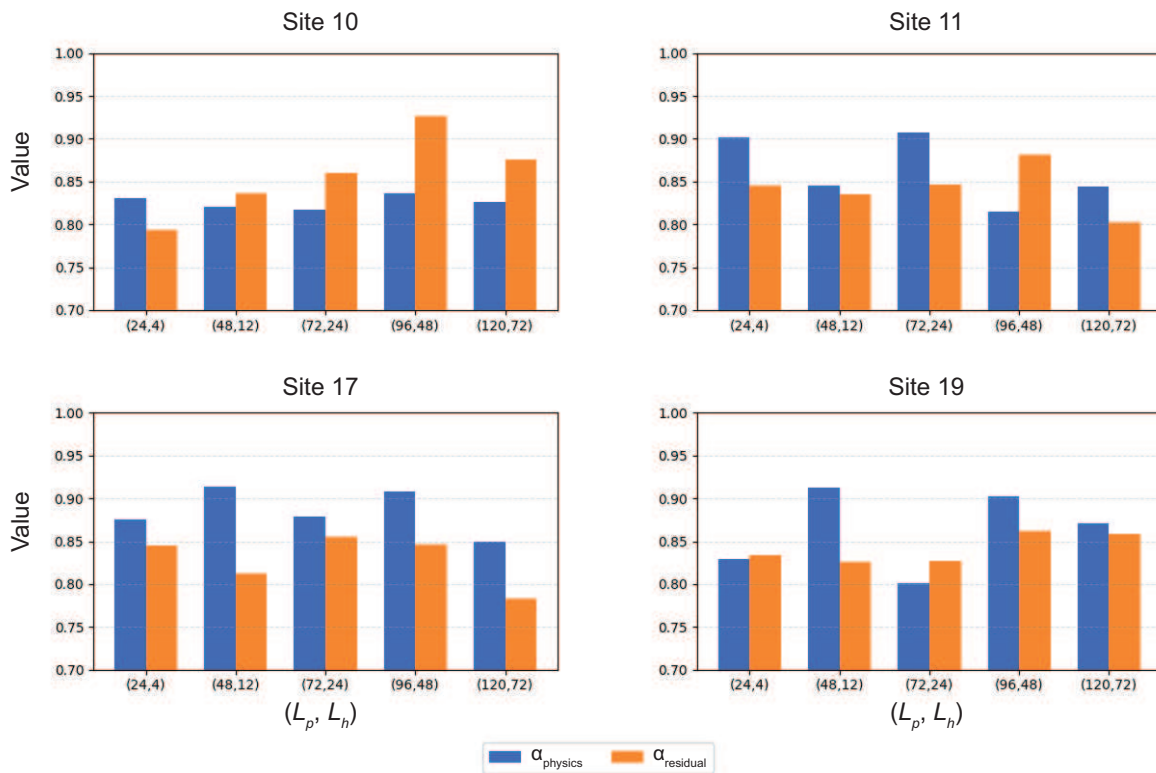


Figure S3. The learned values of $\alpha_{physics}$ and $\alpha_{residual}$ at different sites.

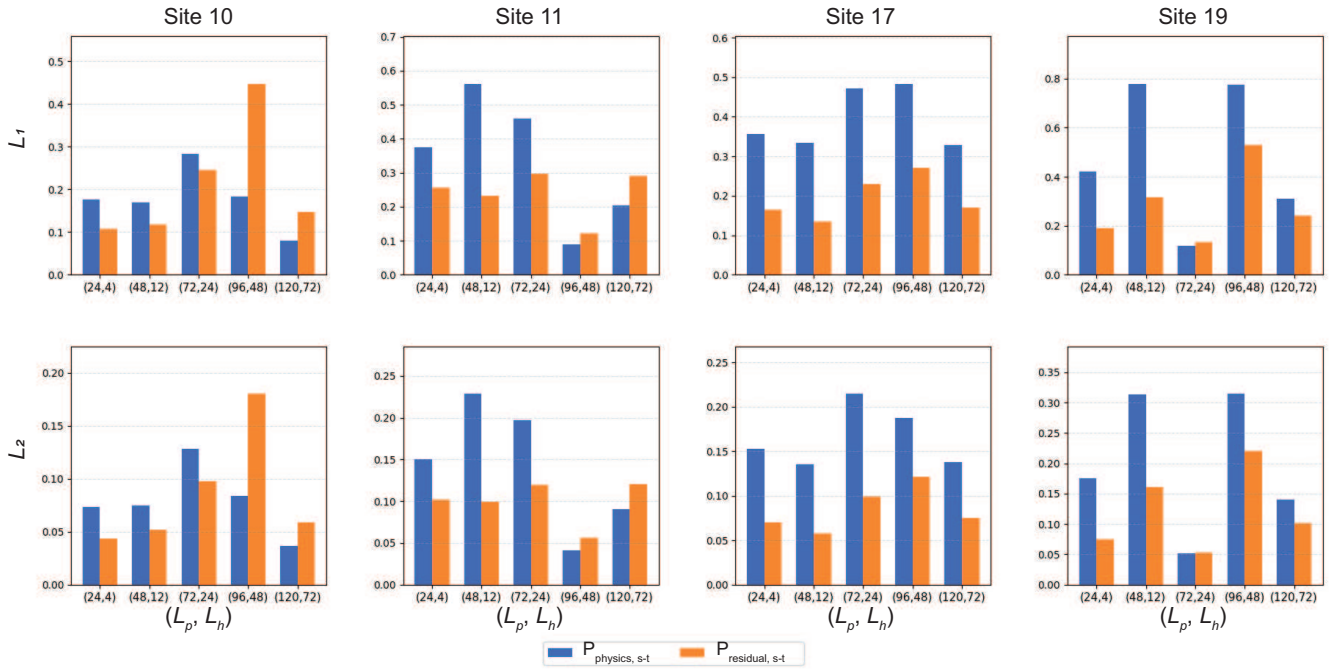


Figure S4. The L_1 and L_2 norms of the B-spline weights at the first KAN module.

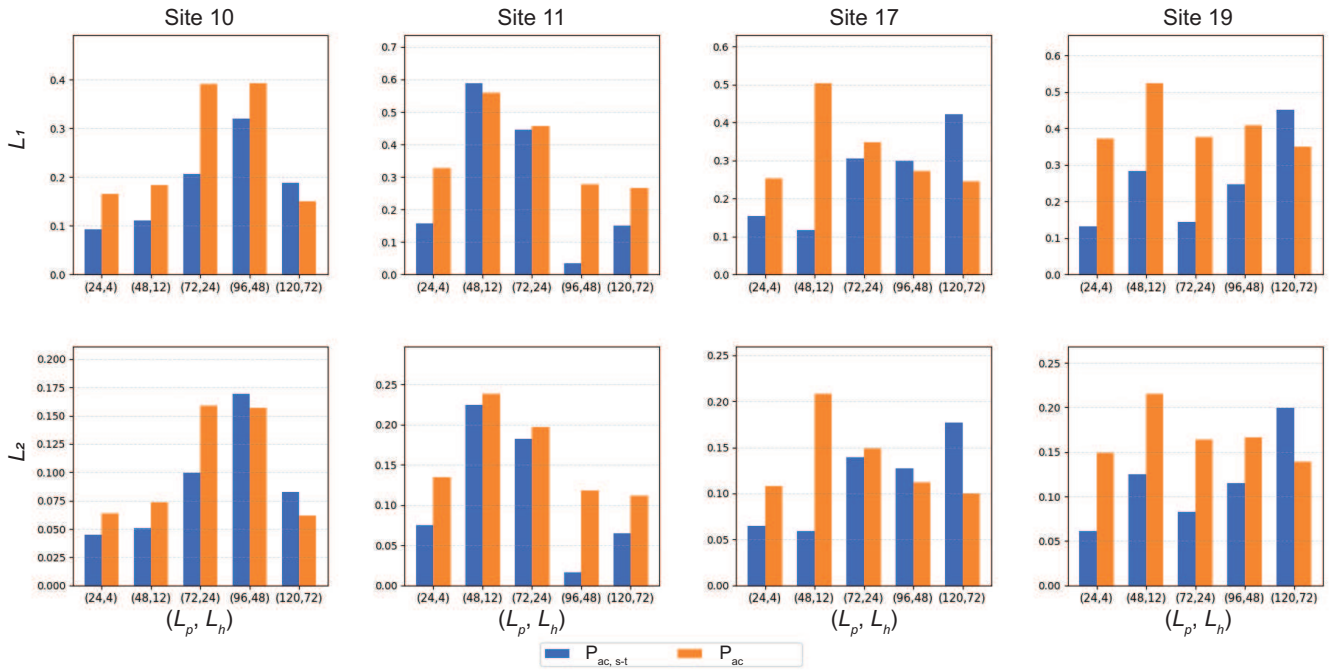


Figure S5. The L_1 and L_2 norms of the B-spline weights at the second KAN module.

Table S3. The ablation experiments for the dataset at site 10

Model	Metric	(L_p, L_h)				
		(24,4)	(48,12)	(72,24)	(96,48)	(120,72)
M1	MAE	0.2730	0.3230	0.3422	0.3949	0.4297
	RMSE	0.5301	0.5739	0.5934	0.6373	0.6826
	R^2	0.8672	0.8446	0.8338	0.8084	0.7800
M2	MAE	0.2733	0.3360	0.3547	0.4279	0.4480
	RMSE	0.5371	0.5742	0.5936	0.6563	0.7059
	R^2	0.8637	0.8444	0.8337	0.7967	0.7647
M3	MAE	0.2758	0.3320	0.3438	0.4902	0.4583
	RMSE	0.5311	0.5773	0.5974	0.6465	0.7087
	R^2	0.8668	0.8427	0.8316	0.8009	0.7629
M4	MAE	0.2852	0.3366	0.3457	0.3965	0.4580
	RMSE	0.5321	0.5793	0.5995	0.6405	0.7073
	R^2	0.8662	0.8417	0.8303	0.8064	0.7638
M5	MAE	0.2751	0.3302	0.3437	0.4094	0.4581
	RMSE	0.5314	0.5770	0.5977	0.6494	0.7079
	R^2	0.8666	0.8429	0.8314	0.8010	0.7634

Table S4. The ablation experiments for the dataset at site 11

Model	Metric	(L_p, L_h)				
		(24,4)	(48,12)	(72,24)	(96,48)	(120,72)
M1	MAE	0.2333	0.2763	0.3023	0.3547	0.3792
	RMSE	0.4484	0.4851	0.5144	0.5587	0.5876
	R^2	0.8719	0.8503	0.8316	0.8015	0.7804
M2	MAE	0.2625	0.2794	0.3147	0.3579	0.3852
	RMSE	0.4595	0.4867	0.5163	0.5624	0.5973
	R^2	0.8654	0.8493	0.8304	0.7988	0.7731
M3	MAE	0.2422	0.2812	0.3031	0.3559	0.3888
	RMSE	0.4490	0.4896	0.5153	0.5599	0.6176
	R^2	0.8716	0.8474	0.8310	0.8006	0.7574
M4	MAE	0.2650	0.2848	0.3141	0.3531	0.3999
	RMSE	0.4574	0.4925	0.5149	0.5575	0.6235
	R^2	0.8667	0.8456	0.8313	0.8023	0.7528
M5	MAE	0.2427	0.2776	0.3023	0.3573	0.3814
	RMSE	0.4491	0.4870	0.5137	0.5605	0.5896
	R^2	0.8715	0.8490	0.8320	0.8002	0.7789

Table S5. The ablation experiments for the dataset at site 17

Model	Metric	(L_p, L_h)				
		(24,4)	(48,12)	(72,24)	(96,48)	(120,72)
M1	MAE	0.3328	0.3937	0.4374	0.4976	0.5396
	RMSE	0.6288	0.6867	0.7315	0.7928	0.8386
	R^2	0.8815	0.8588	0.8398	0.8120	0.7896
M2	MAE	0.3459	0.4079	0.4438	0.5308	0.5482
	RMSE	0.6335	0.6977	0.7335	0.8172	0.8528
	R^2	0.8797	0.8543	0.8389	0.8002	0.7824
M3	MAE	0.3398	0.3994	0.4427	0.5071	0.5494
	RMSE	0.6319	0.6895	0.7319	0.7959	0.8433
	R^2	0.8803	0.8577	0.8396	0.8105	0.7872
M4	MAE	0.3405	0.3998	0.4427	0.4948	0.5485
	RMSE	0.6402	0.6938	0.7347	0.7947	0.8412
	R^2	0.8772	0.8559	0.8384	0.8111	0.7883
M5	MAE	0.3349	0.3997	0.4437	0.4955	0.5479
	RMSE	0.6360	0.6890	0.7322	0.7939	0.8426
	R^2	0.8788	0.8579	0.8395	0.8114	0.7876

Table S6. The ablation experiments for the dataset at site 19

Model	Metric	(L_p, L_h)				
		(24,4)	(48,12)	(72,24)	(96,48)	(120,72)
M1	MAE	0.2328	0.2704	0.3063	0.3491	0.3748
	RMSE	0.4454	0.4844	0.5056	0.5568	0.5875
	R^2	0.8821	0.8606	0.8421	0.8160	0.7950
M2	MAE	0.2420	0.2947	0.3133	0.3553	0.3931
	RMSE	0.4487	0.4885	0.5201	0.5588	0.6017
	R^2	0.8803	0.8583	0.8394	0.8146	0.7850
M3	MAE	0.2377	0.2794	0.3130	0.3512	0.3760
	RMSE	0.4477	0.4865	0.5293	0.5583	0.6027
	R^2	0.8808	0.8594	0.8337	0.8150	0.7843
M4	MAE	0.2369	0.2789	0.3092	0.3526	0.3781
	RMSE	0.4480	0.4911	0.5298	0.5609	0.6092
	R^2	0.8807	0.8568	0.8333	0.8132	0.7796
M5	MAE	0.2349	0.2792	0.3110	0.3512	0.3728
	RMSE	0.4461	0.4861	0.5273	0.5579	0.5950
	R^2	0.8817	0.8697	0.8349	0.8152	0.7898